KSTLE International Journal, Vol. 4, No. 1, June 2003, pp. 31-36

Relationship between Spring Shapes and the Ratio of Wear Volume to the Worn Area in Nuclear Fuel Fretting

Young-Ho Lee†, Hyung-Kyu Kim and Youn-Ho Jung

Korea Atomic Energy Research Institute 150 Dukjin-dong, Yusong-ku, Daejeon 305-353, Korea

Abstract: Sliding and impact/sliding wear test in room temperature air and water were performed to evaluate the effect of spring shapes on the wear mechanism of a fuel rod. The main focus was to quantitatively compare the wear behavior of a fuel rod with different support springs (i.e. two concaves, a convex and a flat shape) using a ratio of wear volume to worn area (D_e). The results indicated that the wear volumes at each spring condition were varied with the change of test environment and loading type. However, the relationship between the wear volume and worn area was determined by only spring shape even though the wear tests were carried out at different test conditions. From the above results, the optimized spring shape which has more wear-resistant could be determined using the analysis results of the relation between the variation of D_e and worn surface observations in each test condition.

Keywords: Sliding and impact/sliding wear, fuel rod, spring shape, ratio of wear volume to worn area

Introduction

Fretting-related degradation generally occurs due to a relatively small displacement between contacting parts and depends on the slip amplitude, environment, contact force and contact shape. In nuclear power plants, especially, the fretting wear phenomenon which frequently occurs between the nuclear fuel rod and its supporting structures (spring or dimple) are mainly caused by flow-induced vibration (FIV), which is generated when the primary coolant rapidly passes around the fuel rod to remove excess heat. In order to restrain these damages, it is essential to design an optimized wear-resistant spring shape because other methods such as coating technology, material replacement, etc, are strictly limited by the consideration of heat transfer and neutron absorption. However, the contact conditions between the fuel rod and springs could be affected by the improvement of the spring shape. So, it is expected to change the wear behavior of a fuel rod with each spring shape and the results of the unexpected wear behavior and mechanism of fuel rod with the modified spring shape should be assessed.

However, the previous experiments in this laboratory have demonstrated that the worn area shape after the wear test was determined by only spring shape and had no connection with the vibration mode and test environment [1,2]. This means that the final volumes of fuel rod with the springs are closely related not only to the shapes of the worn area which are determined by spring shapes but also the maximum depth at each worn area. But, it is not enough to numerically compare the wear volume and maximum wear depth for the evaluation of a wear-resistant spring shape. So, it is necessary to propose a new parameter which correlates the spring shape effect and properties of wear behavior. This will be a great help in the modification, design and development of the next spring shape.

In this paper, sliding and impact/sliding wear tests were performed with Zirconium alloy for four springs with different shape (two concave, convex and flat shapes) in room temperature air and water. As a result, wear properties such as wear volume, worn area and maximum wear depth are analyzed at each test condition and a new parameter (the ratio of wear volume to worn area, D_e) is proposed. The objectives are to compare the wear properties for each spring shape and to verify the application of D_e for the evaluation of the wear-resistant spring shape. The discussion was focused on the spring shape effect and the relationship between D_e at each spring condition and wear behavior.

Experimental details

Specimen

The fuel rod specimen used in this study was Zirconium alloy (abbreviated to Zr-4) and had a 9.5 mm diameter, 0.6 mm thickness by 40 mm long, is cut from the straight rod; this commercial Zirconium-base alloy has been used as nuclear fuel cladding and main components of fuel assembly materials in nuclear power plants. The chemical compositions and mechanical properties are listed in Table 1 and 2. The springs are fabricated by pressing and punching a Zr-4 sheet with a thickness of 0.46 mm. For the variation of the contact conditions, four types of grid spring are used and marked as spring A, B, C and D as shown in Fig. 1. Spring A and C are designed to have a concave contour. So, these springs are wrapped around the tube specimen in a transverse direction of

†Corresponding author; Tel: 82-42-868-8761, Fax: 82-42-863-0565
E-mail: ex-leeyh@kaeri.re.kr

Table 1. Mechanical properties of Zirconium alloy specimen

Yield stress	Tensile strength	Elongation	Elastic modulus	Poissons ratio
344.3 MPa	470 MPa	31%	136.6 GPa	0.294

Table 2. Chemical composition of Zirconium alloy specimen (wt.%)

Zr	Sn	Fe	Cr	O	C	Si
Bal.	1.28	0.22	0.12	0.114	0.013	0.01

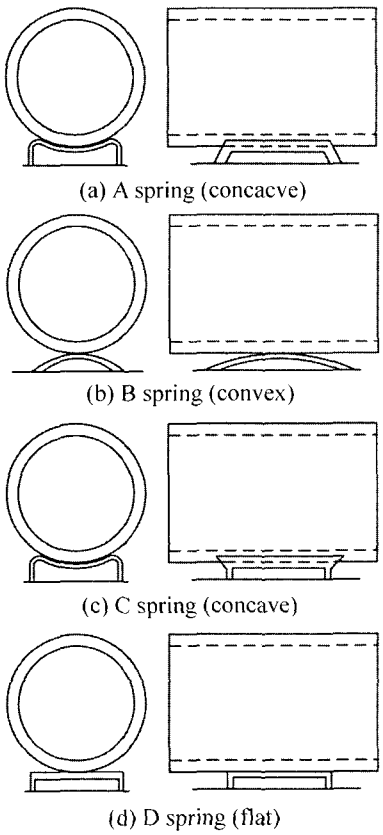

Fig. 1. Schematic diagram of tested specimen.

the contact region. While spring B has a convex contour, so this spring is intended to have a line contact with the tube specimen in its axial length. In contrast to the above springs, spring D has a flat contour. Main difference between the A and C spring is that spring C has a round corner at both spring ends while spring A has a relatively sharp corner with chamfer treatment.

Wear tester

A new high temperature and pressure impact/sliding wear tester was particularly developed for the present works in order to simulate the fretting wear phenomena due to FIV between the fuel rod and spring/dimple in the nuclear power plant environment (above 320°C, 15 MPa). A schematic diagram of the specimen array in an autoclave of this tester is shown in Fig. 2. The fuel rod and spring specimen are attached to the sliding and impact axis, respectively. In addition, the load cells and LVDTs for the high temperature and pressure condition

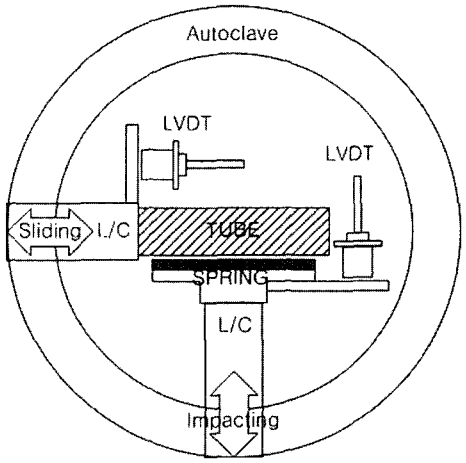

Fig. 2. Specimen array in autoclave.

were equipped at each moving axis to monitor the contact force and slip amplitude.

Test condition

Sliding and impact/sliding wear experiments were performed in room temperature air and water. In this test, various test conditions were selected in order to simulate the fretting wear phenomenon of the fuel rod against the grid spring. The fuel rod specimen equipped in the sliding axis oscillates with a peak-to-peak amplitude of 50, 80 and 100 μm at a frequency of 30 Hz. The normal load of 10 N in the sliding wear test was applied using impact axis. During impact/sliding wear test, maximum impact load was set 10 N with an amplitude of 360 μm at a frequency of 30 Hz. In the water condition, distilled water was used. All wear tests were carried out up to 10^5 cycles at 22 ± 3°C. After the experiment, wear volume and worn area of the fuel rod specimen were measured using a surface roughness tester and an optical microscope, respectively. In this study, loading type and the test environment were abbreviated as follows: sliding in air is SA, sliding in water SW, impact/sliding in air IA and impact/sliding in water IW.

Worn surface observation and area calculation

The worn surface of the fuel rod was examined using an optical microscope to analyze wear particle behavior on the worn area and to calculate the size of the worn area using a commercial software. Also, scanning electron microscopy (SEM) was used to evaluate the wear mechanism in each test condition. Prior to the SEM observation, the specimens were

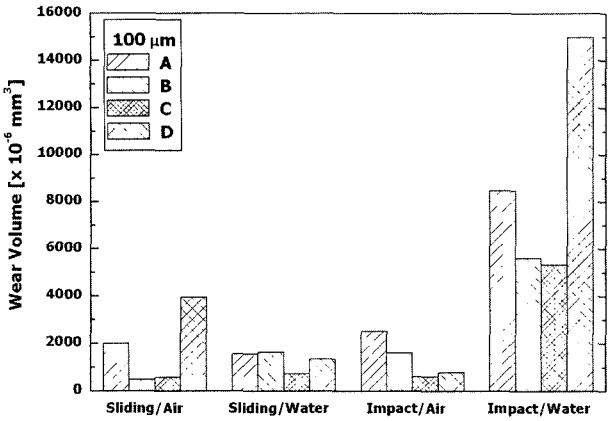

Fig. 3. Variation of wear volume at each test condition.

acoustically cleaned in acetone for 10 min and dried in air.

Results and Discussion

Variation of wear volume

After the sliding and impact/sliding wear test at each test condition, the results of average wear volume at the condition of 10 N of a normal load (or maximum impact load) and 100 μm of a slip amplitude are shown in Fig. 3. In this test, the average wear volume is calculated from the results of two or three experiments of the same test condition. The average wear volumes were varied with spring shape, loading type and test environment. The wear volume of spring A and C with similar concave shape was dramatically increased in the IW condition while the test environment and loading type did not have a significant effect on the wear volume in the other three conditions (SA, SW and IA). However, the wear volume of the convex spring B slowly increased when the test condition was varied from SA to IW. In the condition of spring D which had a flat shape, the severe wear volume in the IW condition met our expectations. However, the lowest wear volume is shown in the IA condition. First of all, wear volume of the SW condition is smaller than that of the SA condition. This result is unexpected because the wear volume of the water condition has always been larger compared with that of the air condition [3,4]. Therefore, it was found that the effect of the environment on the fuel fretting problem could be changed with spring shape.

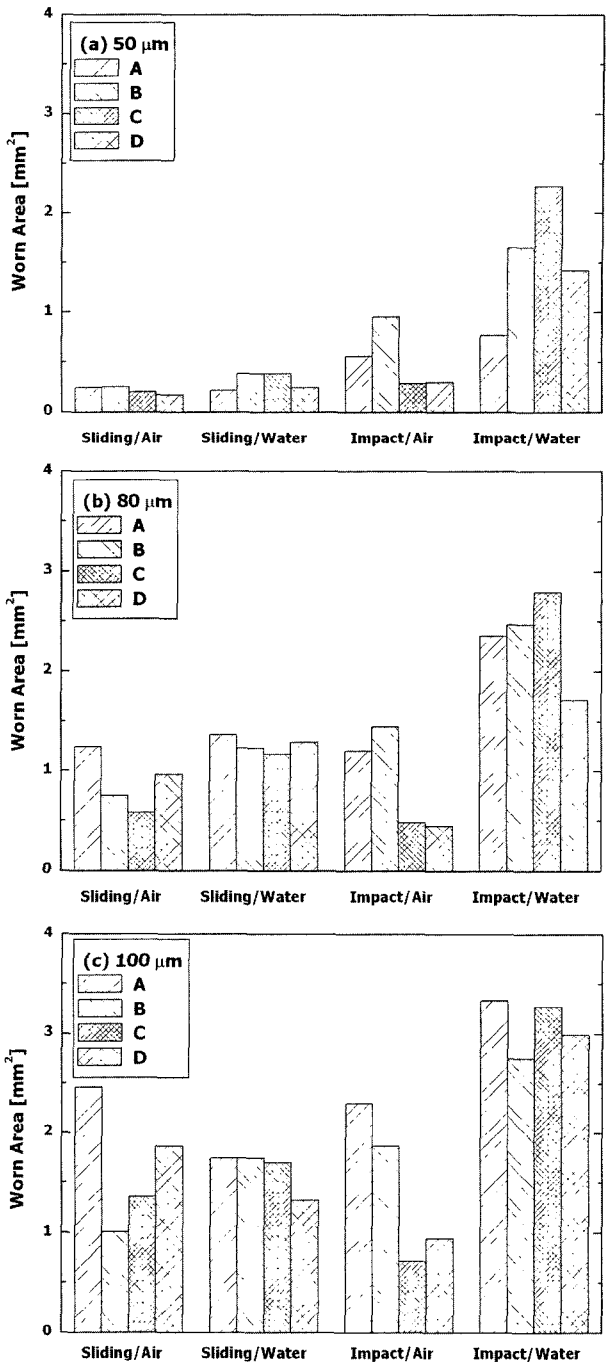

Fig. 4. Comparison of worn area after wear testing.

Worn area

In order to evaluate the different results of wear volume affected by spring shape, test environment and loading type, the size of the worn area was analyzed and calculated. These determine the shape of the worn area which is closely related to the removal and accumulation of wear debris between the contact surfaces during the sliding and impact/sliding wear. Besides, it is very important to compare the shape of the worn area which is finally formed at each test condition because the debris removal path could be varied with the test environment and loading type. As shown in Fig. 4, the variation of the worn area size was similar with volume results, but there are some significant results.

When the test condition changes from sliding in air to impact/sliding in water (namely, SA-SW-IA-IW) at 50 μm, the size of the worn area gradually increased in almost all the spring conditions. But in the 100 μm condition, the difference of worn area size corresponding to the test condition decreased slowly. Especially, area increase in the IW condition with increasing slip amplitude did not markedly accelerate compared with the SA, SW and IA conditions. These results show that the increase of wear volume rapidly progresses rather than the area expansion between the contact surfaces. As

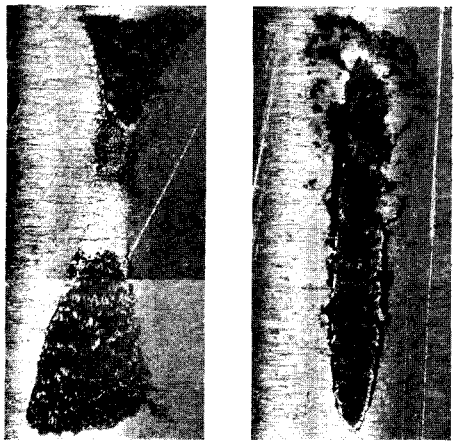

(a) Spring A (100 μm) (b) Spring B (100 μm)

(c) Spring A (100 μm)

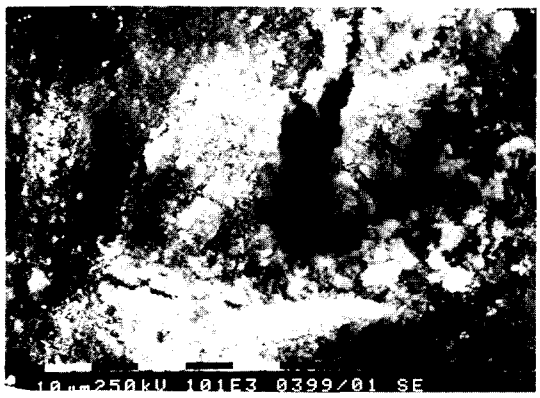

(d) Spring B (100 μm)

Fig. 5. Optical microscope and SEM observation results of worn area after wear test in the IA condition.

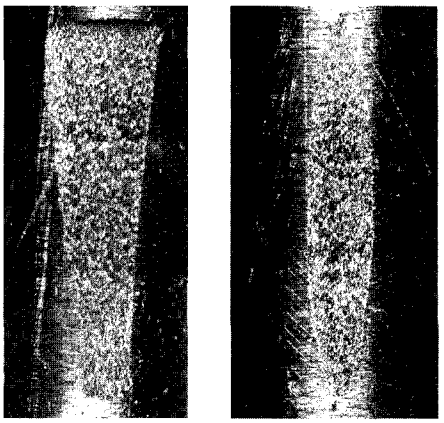

(a) Spring A (100 μm) (b) Spring B (100 μm)

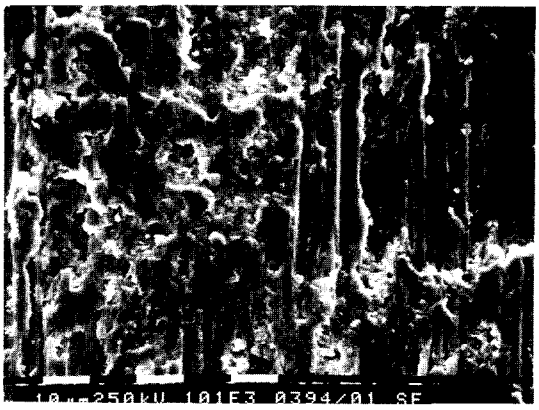

(c) Spring A (100 μm)

(d) Spring B (100 μm)

Fig. 6. Optical microscope and SEM observation results of worn area after wear test in the IW condition.

such, wear mechanism in the IW condition is closely related to the rapid removal of wear debris between the contact surfaces despite the small slip amplitude while that in the SA, SW and IA conditions seems to be governed by debris accumulation between the contact surfaces. Therefore, the behavior of worn area expansion is dominantly determined by slip amplitude in the IW condition while its test environment and loading type in the SA, SW and IA conditions.

Wear progress between the fuel rod and various springs could be divided into interaction between the contact surfaces, wear debris generation/worn area expansion and wear debris removal/wear depth increase. At this time, it is reasonable to suggest that the optimized spring shape should show the slow expansion of the worn area and a restricted removal path of the wear debris. To obtain these parameters at each spring condition, the worn surface was examined using optical microscope and SEM.

Removal of wear debris in impact/sliding test

To investigate the wear mechanism and wear particle behavior

on the worn surface of a fuel rod with various springs, optical microscope and SEM observations were conducted and the results (spring A and B) are shown in Fig. 5 and 6. Under the IA condition, almost all the worn surfaces showed the formation of compacted wear debris but the removal paths of wear debris were determined by the spring shapes. In the case of spring A (Fig. 5(a)), wear debris generated during wear move toward the center area of the contact surface and these with relatively large sizes but became fine debris. During this process, the worn area also expanded into the center of the axial direction and into both ends of the transverse direction. However, spring B condition (Fig. 5(b)) shows that the formation of compacted particle layers compared with spring A condition is expected to play a role in load-bearing layers even though wear debris could be removed in all the directions of the contact surface. Generally, wear particle sizes gradually decreased with increasing interaction time of debris between the contact surfaces. If wear particle sizes are relatively small, they could be easily trapped on suitable sites or accumulated on contact surfaces and finally generate load-bearing layers. As shown in Fig. 5(d), spring B shows relatively smaller particle sizes and more compacted wear particle layers compared with spring A. This means that wear debris could be rapidly fractured because the smaller contact area under the same impact load yields relatively larger contact stress (slip amplitude of 100 μm). This seems to be the main cause of volume difference between spring A and B. On the other hand, in the IW condition as shown in Fig. 6, almost all the wear debris was removed from the worn surface and metal-to-metal contact is more dominant, so the wear mechanism is controlled by deformation and fracture of contact surface.

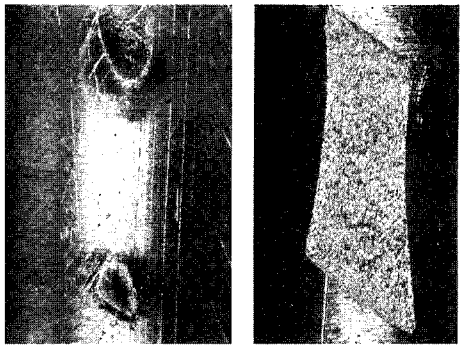

(a) 50 μm, Sliding (b) 50 μm, Impact

Fig. 7. Variation of wear scar at the D spring in the water condition.

From the results of the spring D condition, wear volume in the SA condition is lager than that in the SW condition. In this case, there seems to be a possibility for wear particles remaining on the contact surface. Even if it is expected that the generated wear particles are easily removed in water during sliding, wear particles could be adhered to the worn surface due to the adhesion force and spring shape effect as shown in Fig. 7. In this figure, it is reasonable to suggest that wear debris could be accumulated even in water condition. To obtain a

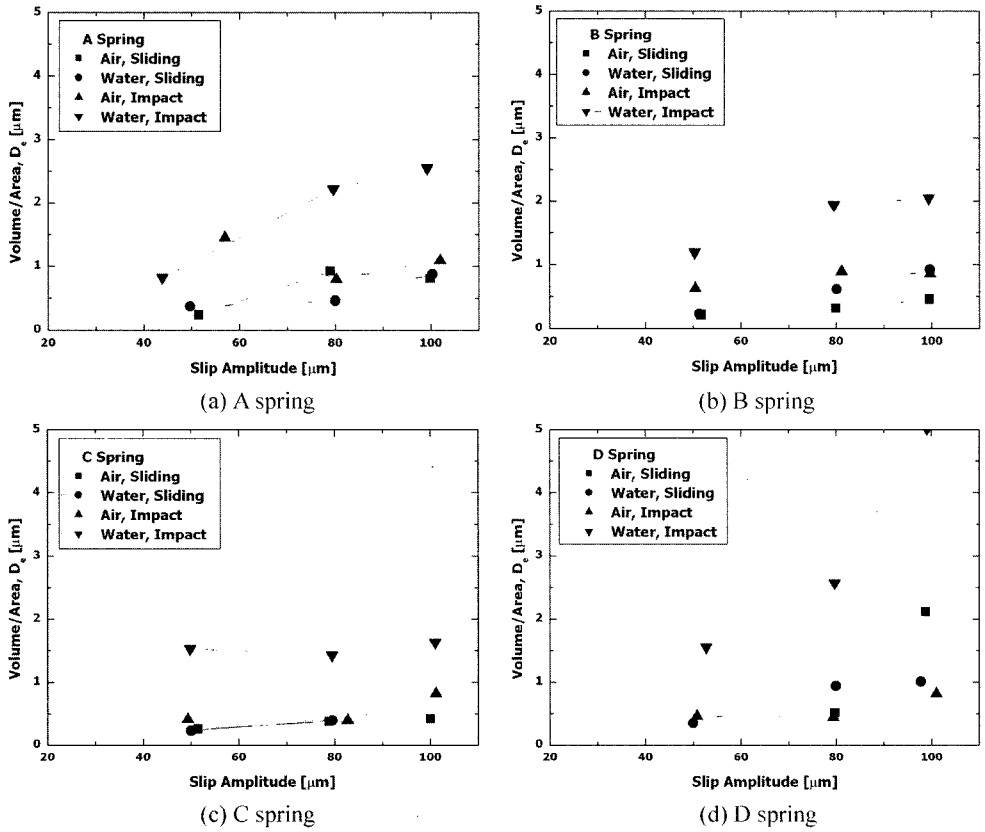

Fig. 8. Variation of the D_e (Volume/Area) at each test spring.

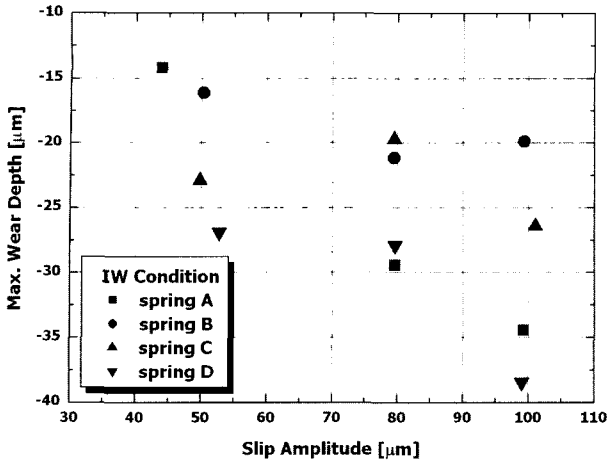

Fig. 9. Variation of maximum wear depth with slip amplitude for each tested spring.

more exact wear mechanism, it is necessary to investigate the adhesion behaviour of wear debris in the water condition in detail.

The ratio of wear volume to worn area (D_e)

From the above results, it is apparent that the shape of the worn area corresponding to the different spring shapes plays an important role in the wear volume of the fuel rod. Among the wear procedures, wear debris removal (volume increase) and worn area expansion (area increase) are directly related to wear damage. So, the ratio of wear volume to worn area (D_e: Equivalent depth = Volume/Area) was considered as the parameter which could compare the wear properties of each spring shape. If D_e is small in a specific spring condition, this means that the area increase is faster than the volume increase, which is connected to a relatively small wear volume and wear depth. In other words, if wear debris generated between the contact surfaces could be accumulated and finally formed as a wear particle layer on the worn surface, wear will progress to the expanded worn area due to the interaction of the removing particles between the fuel rod and spring rather than the increase wear volume in depth direction.

Fig. 8 shows the variation of D_e with slip amplitude at each spring and test condition. In the SA condition, the D_es of spring A and D show a slow increase while those of spring B and C do not change. Especially, in spring C condition, the D_e value does not change with the slip amplitude and test condition except for the IW condition. These trends are in good accordance with the results of wear volume as shown in Fig. 3.

Fig. 9 shows the variation of the maximum wear depth with increased slip amplitude in the IW condition. The maximum wear depth also could be correlated to the relatively lower values of D_e. Therefore, it is reasonable to suggest that the optimized wear-resistant springs show relatively lower maximum wear depth even though they show a larger worn area. In this experiment, spring B and C show a smaller worn area and lower maximum wear depth at the slip amplitude of 100 μm in the IW condition, respectively.

Conclusions

Sliding and impact/sliding wear experiments were performed using a Zirconium alloy nuclear fuel rod for four types of grid springs in room temperature air and water. From those experimental results, the following conclusions are drawn;

(1) The most severe test condition is impact/sliding in water (IW) and spring D which has a flat shape showed the largest wear volume in the IW condition.
(2) It appeared that the effects of the test environment and loading type were changed with the variation of the spring shapes.
(3) Even in the water condition, wear particles can remain between the contact surfaces in the spring with flat shape. This will be discussed in our further study.
(4) It is possible to compare the wear properties of the fuel rod for the various spring shapes using D_e. These results could be applied to design a wear-resistant spring shape.

Acknowledgment

This study has been carried out under the Nuclear R&D Program by Ministry of Science and Technology in Korea.

References

1. Y. -H. Lee *et al.*, "Wear mechanism of tube fretting affected by support shapes," KSTLE International Journal, Vol. 3, p. 68-73, 2002.
2. Y. -H. Lee *et al.*, "Effects of spring shapes on the fuel fretting wear under sliding and impact/sliding load," Proceedings of KNS spring meeting, 2003.
3. Y. H. Lee *et al.*, "A study on wear coefficients and mechanisms of steam generator tube materials," WEAR, Vol. 250, p. 718-725, 2001.
4. Y. H. Lee *et al.*, "The effect of subsurface deformation on the wear behaviour of steam generator tube materials," WEAR, Vol. 253, p. 438-447, 2002.